High-frequency EPR on high-spin transitions-metal sites

Mathies, G.

Citation

Mathies, G. (2012, March 1). *High-frequency EPR on high-spin transitions-metal sites*. *Casimir PhD Series*. Retrieved from https://hdl.handle.net/1887/18552

Author: Mathies, Guinevere
Title: High-frequency EPR on high-spin transition-metal sites
Issue Date: 2012-03-01

Chapter 1

Introduction

The phrase “transition-metal sites” in the title of this thesis refers, on the one hand, to the central metal ion bonded to the ligands in transition-metal complexes. On the other hand it refers to metal centers in proteins and enzymes. The unpaired electrons often found at these transition metals make these sites amenable to study by electron-paramagnetic-resonance (EPR) spectroscopy, which is the main subject of this thesis.

The presence of one or more unpaired electrons results in a net spin angular momentum, which causes a Zeeman splitting of the magnetic sublevels of a transition-metal site by an externally applied magnetic field. For a free electron ($S = 1/2$) the splitting of the states with $m_S = \pm 1/2$ is 9.5 GHz at 340 mT. In a typical EPR experiment the paramagnetic material is placed in a cavity and microwaves are applied at a fixed frequency, usually 9.5 GHz or X band. The absorption of the microwaves is detected as the magnetic field is swept. The magnetic sublevels are influenced by the interaction of the unpaired electrons with their environment and hence the observed EPR spectrum provides information on the electronic structure of the transition-metal site.

In a transition-metal site the ligands affect the d electrons of the transition-metal ion through their electrostatic field and covalent bonding. The degeneracy of the five d orbitals is lifted by the ligand field, in accordance with the rules of group theory. The size of the splitting of the d orbitals depends on the strength of the ligand field. If the splitting is much smaller than the Coulomb and exchange energies of the electrons in the free ion, the ground-state electron configuration will have the highest total spin, consistent with the Pauli exclusion principle. This is called the weak-field or high-spin case. If the splitting becomes larger, it becomes favorable to fill up the low-lying d orbitals. This is the strong-field or low-spin case.

High-spin transition-metal sites show a splitting of the $2S + 1$ magnetic sublevels even if no external magnetic field is applied, the zero-field splitting (ZFS). To optimize the amount of information that can be obtained for these sites by EPR spectroscopy, these sites should be studied at microwave frequencies comparable to or higher than the ZFS. In this thesis we study high-spin Co^{2+} sites, for which this splitting is very large, approaching 1000 GHz, and high-spin Fe^{2+} and Fe^{3+} sites, for which it tends to be more moderate, between 100 - 400 GHz and < 100 GHz, respectively. We set out to do EPR at frequencies higher than the standard 9.5 GHz, which comes with considerable technical difficulties, particularly if one requires the sensitivity needed to study biological materials.

1.1 Electron paramagnetic resonance and the study of transition-metal sites

An electron-paramagnetic-resonance transition can be induced by applying microwaves continuously, continuous-wave (cw) mode, or by applying microwave pulses. In spite of the enormous flexibility and applicability of pulsed EPR techniques and the current strong development in this field, [1] the larger part of this thesis concerns cw EPR. The main reason is that short relaxation times, which make a study by pulsed EPR impossible, are not uncommon in transition-metal sites. A disadvantage of cw EPR is the need to detect the absorption of the microwaves by the paramagnetic sample using lock-in detection. The modulation of the EPR signal is usually created through modulation of the magnetic field. The problems this entails are described in Chapter 2.

The perturbation of the ground state of a paramagnetic site by the interaction of the unpaired electron(s) with their environment and the magnetic field can be captured in a spin Hamiltonian. [2] Depending on the system various terms are incorporated in the spin Hamiltonian to cover all interactions. The strength of the interactions, which is characteristic of the system and may be anisotropic, is represented by usually symmetric interaction “tensors”. The spin Hamiltonian describing the electronic interactions of the unpaired electrons in a transition-metal site should at least contain the following two terms. [3]

$$H_e = \mu_B \vec{B}_0 \cdot \vec{\vec{g}} \cdot \vec{S} + \vec{S} \cdot \vec{\vec{D}} \cdot \vec{S} \tag{1.1}$$

The first term describes the electron Zeeman interaction. The g tensor describes the anisotropic deviation from the free electron value of $g_e = 2.0023$ owing to an orbital angular momentum component contributing to the magnetic moment. The energy levels are perturbed by the spin-orbit coupling, which causes a mixing of the ground state with electronically excited states and partially restores the orbital angular momentum. The second term describes the ZFS, which arises also mainly from the spin-orbit coupling. Because EPR spectroscopy shows transitions between magnetic sublevels, we observe only the anisotropy of this effect. This means that the ZFS tensor can be taken traceless and characterized by two parameters, D and E.

$$D = 3/2 D_z,\ E = 1/2(D_x - D_y) \tag{1.2}$$

D_x, D_y and D_z are the principal values of $\vec{\vec{D}}$. The "rhombicity" of $\vec{\vec{D}}$ is given by the ratio $\lambda = E/D$.

To observe the orientation of the principal axes of an interaction tensor describing a site, it is necessary to study the site trapped in a crystal. The principal values of the interaction, however, may also be obtained from a powder or frozen solution containing all orientations in equal amounts.

Degenerate perturbation theory is used to establish the eigenstates that will result from the perturbation described by the spin Hamiltonian. Thus, the spin Hamiltonian is expressed in a basis of the unperturbed states, $m_S = \pm 1/2, ...$, and diagonalized. The EPR spectrum shows transitions between the eigenstates of the spin Hamiltonian.

Kramers' theorem states that no electrostatic interaction can completely lift the degeneracy of a system containing an odd number of electrons. [4] As a consequence, the sublevels of a half-integer spin system, $S = 1/2, 3/2, 5/2, ...$, will be split in zero field in so-called Kramers doublets.

The behavior of the four magnetic sublevels of a high-spin Co^{2+}, $S = 3/2$, system between 0 and 0.5 T is shown in Figure 1.1. The X-band transitions are shown by vertical lines. In the field range plotted $\vec{S} \cdot \vec{\vec{D}} \cdot \vec{S} \gg \mu_B \vec{B}_0 \cdot \vec{\vec{g}} \cdot \vec{S}$. The eigenvalues and eigenvectors of the dominant ZFS term can be calculated analytically. Two Kramers doublets are found, which are separated in energy by $2\sqrt{D^2 + 3E^2}$.

$$\begin{aligned} |\pm 3/2\rangle &= \cos\theta |3/2, \pm 3/2\rangle + \sin\theta |3/2, \mp 1/2\rangle \\ |\pm 1/2\rangle &= \cos\theta |3/2, \pm 1/2\rangle - \sin\theta |3/2, \mp 3/2\rangle \end{aligned} \tag{1.3}$$

where $tg2\theta = \sqrt{3}E/D$. Although m_S is not a "good" quantum number, the two doublets are referred to as $\pm 3/2$ and $\pm 1/2$. "Forbidden" transitions may occur, i.e. transitions that following the qualification of the doublets by m_S do not seem to obey the selection rule $\Delta m_S = \pm 1$.

The Zeeman interaction can be treated as a perturbation on top of the ZFS. The Zeeman term is expressed in a basis of the states given by Equation 1.3 and diagonalized. The result is referred to as the effective $S' = 1/2$ approximation: each of the two doublets can be described by an effective g' tensor. [7] The principal values of this tensor depend on the g-values and λ, but not on D, cf. Chapters 3 and 4.

If a high-spin Fe^{3+}, $S = 5/2$, system is studied at X band, the microwave quantum is not yet large enough to induce inter-doublet transitions, but the effective $S' = 1/2$ approximation starts to break down. However, the high-field limit, $\vec{S} \cdot \vec{\vec{D}} \cdot \vec{S} \ll \mu_B \vec{B}_0 \cdot \vec{\vec{g}} \cdot \vec{S}$, comes within the reach of the experimentalist. At high magnetic fields the Zeeman term dominates, which means that, with B_0 in the z direction, m_S is almost a "good" quantum number. Subsequently, the ZFS term may be taken into account using first-order perturbation theory since the degeneracy of the states is

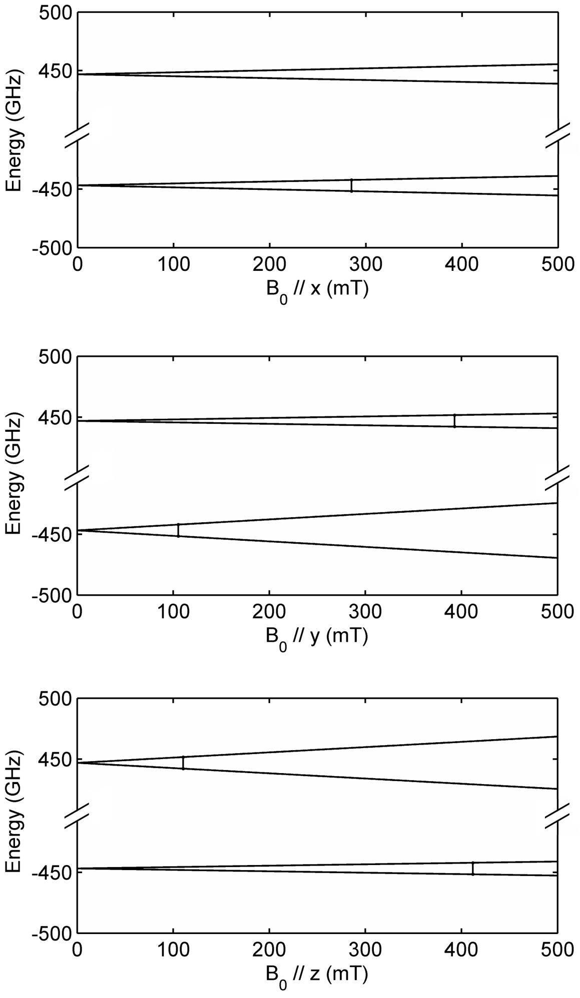

Figure 1.1: The dependence of the energy of the four magnetic sublevels of a high-spin Co^{2+} system, $S = 3/2$, on the magnitude of the magnetic field applied along the x, y and z principal directions of the g and ZFS tensor, which are assumed to be collinear. The example is that of the coordination complex $Co[(SPPh_2)(SP^iPr_2)N]_2$, see Reference [5] and Chapter 4. To calculate the energies of the magnetic sublevels the spin Hamiltonian was diagonalized numerically using the EPR simulation package EasySpin. [6] Because $\lambda = 1/3$ for this system the sign of D remains indeterminate. It was, however, taken positive to create these level plots. The vertical lines show 9.5 GHz resonances.

already completely lifted. As a result allowed, equidistant transitions are expected, the distance being determined by the principal values D_i, cf. Chapters 2 and 6. Figure 1.2 shows the behavior of the six magnetic sublevels of a high-spin Fe^{3+} system between 0 and 12 T. Transitions of 275.7 GHz (J band) are shown by vertical lines: the solid lines represent allowed transitions, which occur only at high fields, the dashed lines represent forbidden transition, which occur at lower fields.

High-spin Fe^{2+} has an integer spin, $S = 2$. The degeneracy of the magnetic sublevels may be completely lifted in zero field and as a result many high-spin Fe^{2+} systems are EPR silent at X band. However, at J band multiple transitions are expected to show up. The energies and composition of the magnetic sublevels can be calculated analytically in zero field, cf. Chapter 5. To calculate the behavior of the sublevels at magnetic fields at which J-band transitions become possible the spin Hamiltonian in Equation 1.1 must be diagonalized numerically.

A hyperfine interaction with a nearby nuclear spin, I, will split the magnetic sublevels according to the possible values of m_I. For instance in the 5 K spectrum in Figure 3.3 in Chapter 3, a splitting of about 4 mT due to the interaction with the cobalt nucleus, $I = 7/2$, is partially resolved. Small splittings may be hard to resolve in an EPR spectrum, but electron nuclear double resonance (ENDOR) can help. As the magnetic field is set to an EPR resonance radio waves are applied. The radio frequency is swept, and if a resonance with the splitting induced by the combined hyperfine *and* nuclear Zeeman interactions is hit the intensity of the observed EPR transition will change. The following nuclear spin Hamiltonian is used to analyze the ENDOR spectra

$$H_n = -\gamma_N \vec{I} \cdot \vec{B} + \langle \vec{S} \rangle \cdot \vec{\vec{A}} \cdot \vec{I} \tag{1.4}$$

The mixing by the hyperfine interaction of the electron-spin states is assumed to be negligible, which justifies the use of the expectation value of the electron-spin angular momentum, cf. Chapter 4.

Transition-metal sites in proteins and enzymes play an essential role in many biological processes. The relation between the (geometric) structure, electronic structure and function of these active sites is studied in bioinorganic chemistry, and EPR spectroscopy is one of its most important tools.

The starting point is the observation of EPR spectra of these transition-metal sites and the interpretation in terms of their spin-Hamiltonian parameters. In the case of high-spin sites it is advantageous, or required, to record EPR spectra at microwave frequencies higher than the standard 9.5 GHz. Even if the technical challenges of generating microwave radiation at these high frequencies and the required high magnetic fields are overcome, the observation and analysis of these spectra is not straightforward, as will become clear in Chapters 2 and 3.

Once the spin-Hamiltonian parameters, which characterize a transition-metal site, are obtained, one would like to translate them into the molecular wave functions. This step requires advanced quantum-chemical calculations. [8] Significant progress has been made the last decade, particularly using density-functional-theory (DFT). However, the translation of the ZFS term is still problematic.

Progress in the calculation of ZFS parameters requires calibration by experi-

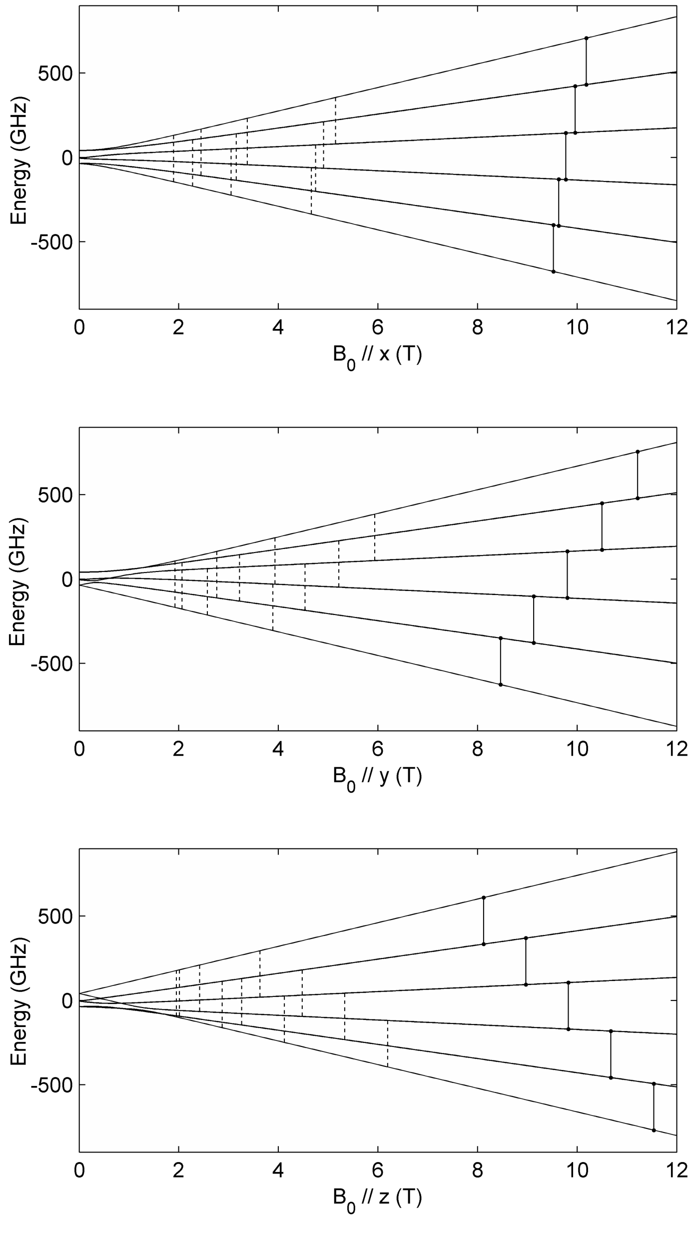

Figure 1.2: The dependence of the energy of the six magnetic sublevels of a high-spin Fe^{3+} system, $S = 5/2$, on the magnitude of the magnetic field applied along the x, y and z principal directions of the g and ZFS tensors, which are assumed to be collinear. [6] The example is that of an iron ion bound to the N-lobe of human serum transferrin, see Chapter 6. The vertical lines show 275.7 GHz resonances. The dashed resonances are “forbidden” transitions.

mentally observed ZFS parameters in different molecular environments. To avoid complications arising in the observation and analysis of EPR spectra of metalloproteins, it is helpful to study biomimetic model complexes, examples of which are reported in Chapters 4 and 5.

1.2 Thesis outline

When the Leiden 275.7 GHz or J-band EPR spectrometer was first taken into operation in 2004 [9] it was equipped with a multi-purpose probe head, suitable for operation in both pulsed and cw mode, and moreover, the cavity had slits to allow optical illumination and ENDOR. The sensitivity and signal stability that could be achieved with this probe head were not sufficient to detect in cw mode the broad resonances of frozen solutions of high-spin metalloproteins. Chapter 2 describes the development of a probe head for the Leiden J-band EPR spectrometer specialized for operation in continuous-wave (cw) mode, which meets these requirements.

To illustrate the possibilities of the J-band spectrometer with the new, cw probe head, spectra are recorded of frozen solutions of the high-spin Fe^{3+} protein rubredoxin [10] from three different organisms: *Desulfovibrio gigas*, found in a small inland sea in the south of France, [11] *Pyrococcus furiosus*, first isolated from geothermally heated marine sediments with temperatures between 90 and 100 °C, [12] and *Megasphaera elsdenii* found in the intestines of cattle. [13] Due to the different environments in which these microorganisms live, the structure of these rubredoxins varies considerably. [14] [15] The structure of the active site, however, hardly differs, and we have found that the same is true for the electronic structure of the sites. The differences in the ZFS parameters are on the order of 1 GHz, which illustrates the close relation between the electronic structure and the function of the active site.

In Chapter 3 the protein desulforedoxin, which is related to rubredoxin, is studied with cw EPR at multiple frequencies. The active site of this protein is studied both in its natural high-spin Fe^{3+} form and substituted with high-spin Co^{2+}. Remarkable differences in electronic structure between the active sites of desulforedoxin and rubredoxin are observed, which are related to the differences in structure and undoubtedly to the function of the active sites.

In Chapter 4 of this thesis the full hyperfine tensors of the four phosphorus nuclei, $I = 1/2$, in the high-spin Co^{2+} complex $Co[(SPPh_2)(SP^iPr_2)N]_2$, previously characterized by multi-frequency EPR, [5] are determined by pulsed ENDOR at 94.9 GHz (W band). These hyperfine tensors are found to depend on whether two phenyl (Ph) or two isopropyl (^{i}Pr) groups are bonded to the phosphorus atom. Thus, the Co−S bonds are non-equivalent as a result of a subtle difference relatively far away from the $Co(II)S_4$ core.

In Chapter 5 the high-spin Fe^{2+} complex $Fe[(SPPh_2)_2N]_2$ is studied by cw EPR at 9.5, 94.1 and 275.7 GHz. Powder spectra at W band and J band showed the presence of two molecules with a slightly different electronic structure near the iron ion. Spectra recorded at J band on a crystal made it possible to distinguish the signals arising from the two molecules and their spin-Hamiltonian parameters could be determined with high accuracy.

Chapter 6 describes the results of cw EPR at J band on transferrin, a protein that plays an important role in the iron metabolism of all vertebrates. [16] Most transferrins consist of two homologous lobes each containing a deep cleft capable of strong, but reversible binding of a high-spin Fe^{3+} ion. In the research on transferrin EPR has been used, but not nearly to a full extent, because at X band the information that can be obtained on a high-spin Fe^{3+} site is limited. The two lobes are not distinguished and, moreover, the characteristic X-band spectrum of transferrin is not quantitatively understood. At J band the two lobes are distinguished in the spectrum of human serum transferrin and the spectrum is satisfactorily reproduced by simulation. The observation of the signals due to the two lobes is supported by spectra recorded on two monoferric forms of human serum transferrin in which either of the binding sites is disabled by a local mutation.

The final chapter of this thesis does not deal with EPR on transition-metal sites. Instead resonance Raman spectroscopy is employed to observe the vibrational modes of spheroidene in the photosynthetic reaction center (RC) of *Rhodobacter sphaeroides*. This carotenoid is believed to have a photoprotective function, although the exact mechanism is not understood. In literature no consensus existed on the configuration of the spheroidene molecule in the RC. Using as a calibration resonance Raman spectra obtained on isotope labeled spheroidene, reconstituted into the RCs of the carotenoidless mutant of *Rb. sphaeroides* R26, a method to calculate the resonance Raman spectra of spheroidene in a particular conformation has been developed in the last decade. [17, 18] In Chapter 7 resonance Raman spectra detected at different excitation wavelengths of wild-type RCs are compared to those of reconstituted R26 RCs. Combining these spectra with the calculations allowed us to establish the configuration of spheroidene in the RC of wild-type *Rb. sphaeroides* to be 15,15′-*cis*. However, in the reconstituted R26 RCs spheroidene occurs in two configurations, namely 15,15′-*cis* and 13,14-*cis*.